The Journal of Arthroplasty xxx (2019) 1–7

Contents lists available at ScienceDirect

The Journal of Arthroplasty

journal homepage: www.arthroplastyjournal.org

Analysis of Biomechanical Differences Between Condylar Constrained Knee and Rotating Hinged Implants: A Numerical Study

Lorenzo Andreani, MD [a], Silvia Pianigiani, PhD [b], Edoardo Bori, MS [b], Michele Lisanti, MD [a], Bernardo Innocenti, PhD [b,*]

[a] *Orthopaedic and Trauma Unit, University of Pisa, Pisa, Italy*
[b] *BEAMS Department (Bio Electro and Mechanical Systems), Université Libre de Bruxelles, Brussels, Belgium*

A R T I C L E I N F O

Article history:
Received 21 May 2019
Received in revised form
17 July 2019
Accepted 1 August 2019
Available online xxx

Keywords:
revision TKA
tibial stress
implant micromotions
condylar constrained implant
rotating hinged implants

A B S T R A C T

Background: Different levels of constraint for total knee arthroplasty can be considered for revision surgeries. While prior studies have assessed the clinical impact and patient outcomes of condylar constrained knee (CCK) and rotating hinged (RTH) implants, nowadays little is known about the biomechanical effects induced by different levels of constraint on bone stress and implant micromotions.

Methods: CCK and RTH implant models were analyzed using a previously validated numerical model. Each system was investigated during a squat and a lunge motor task. The force in the joint, the bone and implant stresses, and micromotions in this latter were analyzed and compared among designs.

Results: Different activities induced similar bone stress distributions in both implants. The RTH implant induces mostly high stress compared to the CCK implant, especially in the region close to tip of the stem. However, in the proximal tibia, the stresses achieved with the CCK implant is higher than the one calculated for the RTH design, due to the presence of the post-cam system. Accordingly, the condylar constrained design shows higher implant micromotions due to the greater torsional constraint.

Conclusion: Different levels of constraint in revision arthroplasty were always associated with different biomechanical outputs. RTH implants are characterized by higher tibial stress especially in the region close to the stem tip; condylar implants, instead, increase the proximal tibial stress and therefore implant micromotions, as a result of the presence of the post-cam mechanism. Surgeons will have to consider these findings to guarantee the best outcome for the patient and the related change in the bone stress and implant fixation induced by different levels of constrain in a total knee arthroplasty.

The increasing number of patients undergoing primary total knee arthroplasty (TKA; 720,000 in the USA during 2010) has been accompanied by a similar increase in the number of revision TKAs (70,000 in the USA during 2011) [1–3]. One study estimated the overall incidence of primary and revision TKA to grow by 174% and 600%, respectively, between 2005 and 2030 [4]. One of the major challenges of TKA is the management of instability, a factor which is a prerequisite for postoperative function as well as implant survival [5]. Overcoming soft-tissue instability requires a challenging combination of managing ligament deficiency, balancing the flexion and extension gaps, and handling extensor mechanism insufficiency [6]. Indeed, different levels of constraint for TKA can be considered for revision surgeries because both semiconstrained and hinged implants guarantee more stability than primary TKA implants. The selection of the correct constraint level is therefore of paramount importance in this context [7,8].

Hinged knee prostheses with a fixed axis were introduced to restore knee function and correct limb alignment in the presence of severe malalignment and/or instability [9]; this type of prosthesis is a linked constrained device able to provide the highest level of constraint, therefore conferring stability on coronal plane, on sagittal plane, and in rotation. High failure rate in the first generation of these implants [9,10] has highlighted the need for further studies and improvements, thus leading to the rotating hinged (RTH) implants; introduced in 1982 [11], they are typically used in case of

No author associated with this paper has disclosed any potential or pertinent conflicts which may be perceived to have impending conflict with this work. For full disclosure statements refer to https://doi.org/10.1016/j.arth.2019.08.005.

* Reprint requests: Bernardo Innocenti, PhD, BEAMS Department (Bio Electro and Mechanical Systems), Université Libre de Bruxelles, Av. F. Roosevelt, 50 CP165/56, 1050 Brussels, Belgium.

https://doi.org/10.1016/j.arth.2019.08.005
0883-5403/

ligament absence or disruption in combination with moderate or severe bone loss, poor soft-tissue envelope, and severe varus-valgus and flexion contracture [5,12–16], allowing the physiological knee motion to be restored, thanks to the feasibility of the so-called home-screw mechanism [17]. Compared to first-generation hinged TKAs, decrease in loosening rates and improvements in gait pattern have been achieved in RTH implants [18,19]; a potential advantage of this design is furthermore the reduction in shear stresses around the bone-cement interface due to the additional rotational degree of freedom around the tibial axis [20,21]. Studies reporting clinical outcome of different types of RTH implants have been published, some of them with controversial conclusions [16,19,22–25].

Condylar constrained knee (CCK) prostheses are instead semi-constrained, nonlinked implants which, thanks to an apposite post-cam mechanism (like the posterior-stabilized implant but bigger and thicker), confer different level of varus-valgus and rotational stability depending on the post-cam engagement design (specific for each manufacturer) [26]. CCK systems have been introduced more recently and are generally assumed to be less constrained than RTH designs, so their use has become increasingly popular as the alternative to the hinged prostheses in cases of intermediate severity [5]. This design is characterized by a wide and long tibial post engaging the large and deep intercondylar cam of the femoral component, thus ensuring mediolateral and rotational stability without constraining the anteroposterior direction [27,28]. They can be preferable to hinged TKA in case of medial and/or lateral collateral ligament insufficiency and limited bone loss [29–31]. However, in presence of severe flexion instability or collateral ligament deficiency, potential post-cam dislocation (as in posterior-stabilized implants [12,32]) must be taken into account and a hinged TKA could be considered a better option.

Clinical studies have shown that when implant selection is guided by inherent stability of the knee, CCK and RTH knee designs have similar outcomes [6]; Fuchs et al [33] found no significant differences in terms of Hospital for Special Surgery Score, Knee Society Score, Pain and Tegner score in their retrospective cohort study, while standard condylar revision implants yielded better postoperative mobility but had a lower Short Form 36 Mental Component Score: this latter finding may then imply that patients tolerate the RTH design better than the standard condylar revision implant [7]. Walker et al [34] also compared the RTH design with standard condylar revision in a cohort study, finding a high correlation in performance between the operated and nonoperated side in the RTH group, thus indicating the hinges as capable of matching the nonoperated knee performance.

However, even if prior studies have assessed the clinical impact and patient outcomes of CCK and hinged implants, nowadays little is known about the biomechanical effects induced by different levels of constraint. For this reason, the aim of the study is to analyze and compare a semiconstrained and a hinged TKA implant during different motor tasks. In particular, bone stresses and implant micromotions were investigated using a previously validated numerical approach [35,36] and a comparison among the different implants was performed.

Materials and Methods

This study was conducted developing a numerical model coupling rigid body kinematics and finite element (FE) model. The model developed for this study was based on an already validated and published knee FE model [36] including the following features.

Geometry

A physiological 3-dimensional tibial bone model was created from computer tomography images of a fourth-generation composite left tibia, medium size (# 3401, Sawbones; Pacific Research Laboratories Inc, Malmo, Sweden); such models are widely used for numerical and experimental tests, as reported in the literature [37–39]. The tibial bone model consists of 3 parts: cortical bone, cancellous bone, and the intramedullary canal.

As revision TKA solutions, the Legion Revision Condylar Constrain Knee (Smith & Nephew, Memphis, TN) and the RT-PLUS Rotating Hinged prostheses (Smith & Nephew, Memphis, TN) were taken respectively as CCK and RTH implants. The CCK implant used constrains, as reported by previous study [28], varus-valgus, and internal-external rotations together with mediolateral translation.

According to the dimensions of the tibial bone model used, a size 6 tibial tray with a 9-mm polyethylene insert was selected for the CCK solution, while a size 4 tibial tray with an 8-mm polyethylene insert was selected for the hinged solution. In order to verify the correct choice of the TKA components and their positioning, an actual implant surgery was performed, using the suitable devices and instrumentation, by an experienced orthopedic surgeon (L.A.) on real mechanical-equivalent synthetic tibias. For both revision TKA models, a 160-mm stem with a 12-mm diameter was selected, but nevertheless the design of the 2 stems was not completely equivalent as the one adopted for the CCK presented a slot while the other was unslotted. This choice of equivalent dimensions for the stems was made in order to allow a direct comparison of the results [35,40–42].

Two replaced models (one for each type of prosthesis) were then generated: following the manufacturer's recommendations and the in vitro implant procedure, both designs were used to virtually replicate the surgical procedure on the validated knee model. To ream the intramedullary canal, numerical models of the surgical rasps were virtually created, to exactly reproduce all the steps of the actual implantation procedure. To define the position of the stem in the numerical models, the cortex engagement of 3 edges of the stem was recognized [28].

Material Models and Properties

The materials considered in this study were assumed to be homogeneous, isotropic, and linear elastic [36,43,44]; the properties assigned to femoral component, tibial insert, and tibial tray were respectively the ones of cobalt-chromium alloy (CoCr), of ultra-high-molecular-weight polyethylene, and of titanium alloy (Ti6Al4V). According to the literature, the cortical bone was considered transversely isotropic with properties varying along the mechanical axis of the tibia; the cancellous one was instead assumed to be homogeneous, isotropic, and linear [36,37,39,45,46]. The material properties of the knee model used in this study are reported in Table 1. A cement layer with a constant penetration of 3

Table 1
Material Properties Used for the Different Components of the Model.

Material	Material Models	Elastic Modulus (MPa)			Poisson's Ratio		
		E_1	E_2	E_3	ν_{12}	ν_{13}	ν_{23}
Cortical bone	Transversely isotropic	10,000	10,000	16,000	0.42	0.3	0.3
Cancellous bone	Isotropic	3000	—	—	0.3	—	—
Ti6Al4V	Isotropic	110,000	—	—	0.3	—	—
CoCrMo	Isotropic	248,000	—	—	0.3	—	—
UHWMPE	Isotropic	564	—	—	0.23	—	—
PMMA	Isotropic	3000	—	—	0.3	—	—

All materials are considered homogeneous, isotropic linear behavior, with exception of cortical bone that is considered orthotopic with the third axis parallel to the anatomic axis of the bone.
Ti6Al4V, titanium alloy; CoCrMo, cobalt-chromium alloy; UHMWPE, ultra-high-molecular-weight polyethylene; PMMA, poly(methyl methacrylate).

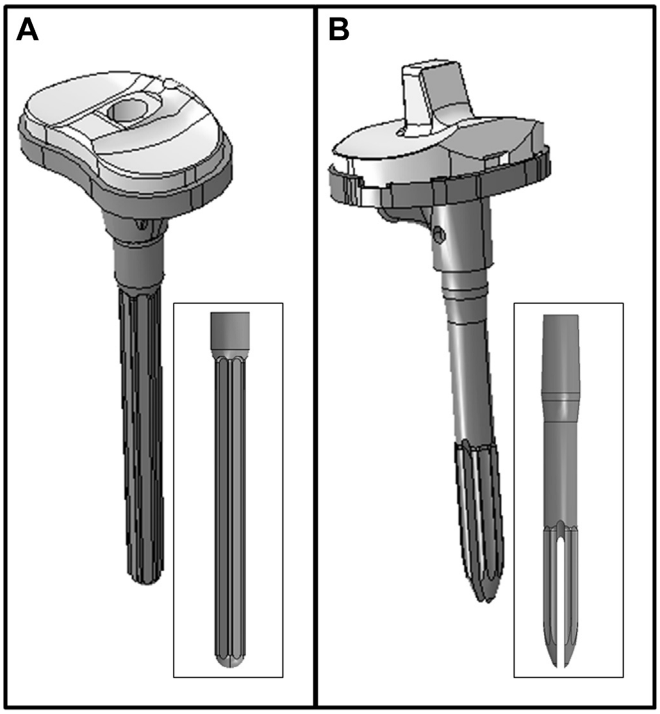

Fig. 1. Tibial components of the TKA designs used for this study: (A) hinged design; (B) semiconstrained design. The box at the bottom right reports the details of the stem for each design. TKA, total knee arthroplasty.

mm into the bone (based on a test of different cementing techniques [47,48]) was applied at the interface between the tibial bone cut and the tibial component; the material adopted for the cement was homogeneous and isotropic [39,45,46].

According to previous studies, the coefficient of friction between the insert and the tibial tray was 0.05, between the titanium stem (press-fit) and bone was 0.6, and between the CoCrMo (tibial tray and cemented stem) and bone was 0.2 [40,49].

Kinematic Analysis of Different Motor Tasks

Lunge and squat movements were numerically reproduced using a validated musculoskeletal modeling software (LifeMOD/KneeSIM 2008.1.0; LifeModeler Inc, San Clemente, CA) [50,51]. This model is able to replicate an existing knee kinematics rig with regard to geometry, constraints, input, and output. Squat and lunge movements were implemented with a range of flexion from 0° to 120° and 90°, respectively. A constant vertical hip load of 200 N was applied during both the motor tasks in order to allow a proper comparison among the results. All other settings and hardware parameters necessary to define rigid body kinematics were based upon prior studies [39,50,52].

Medial and lateral tibiofemoral contact forces, patellar tendon forces, and implant tibiofemoral kinematics during both activities were extracted. Implant kinematics were reported following the Grood and Suntay convention [53].

FE Analysis

Each revision TKA model was meshed by using tetragonal elements with an approximate element size of 4 mm. A refinement of the mesh, with an approximate element size of 0.5 mm, was performed in the contact region between bone and the TKA stem. The proper size of the elements was chosen after a convergence test

Table 2
Kinematic Results of the Hinged and CCK TKA in Terms of Max Flexion, Max Abduction, and Max Internal-External Rotation for Lunge and Squat Motor Task.

Activity	Flexion	Abduction	Internal-External
Hinged TKA			
Lunge	88.4°	0.7°	8.3°
Squat	118.8°	0.6°	6.2°
CCK TKA			
Lunge	90.9°	0.0°	0.5°
Squat	119.3°	−0.4°	−0.4°

All the values reported in the table are in degrees.
CCK, condylar constrained knee; TKA, total knee arthroplasty.

performed to verify that the mesh size adopted did not affect the requested outputs. Abaqus/Standard version 6.10-1 (Dassault Systèmes, Vélizy-Villacoublay, France) was used to develop the models and to perform all the analyses.

The maximum tibiofemoral forces (medial and lateral) resulting from the kinematic analysis of the different motor tasks were used as inputs for loads and boundary conditions in the FE simulations; similar process was adopted for the hinged prosthesis, where the joint internal forces were determined by the rigid body analysis and then applied to the implant, and for the CCK implant, calculating the post-cam force to be applied on the polyethylene insert. For all models and motor tasks, patellar tendon force was applied on the tibial tubercle and the tibia was fully constrained distally.

Twenty regions of interest (ROIs) were identified in the tibia subdividing its cortical section in 10-mm-thick regions (see Fig. 1), defined by cutting the cortical bone with planes perpendicular to the mechanical axis of the tibia and therefore parallel to the proximal tibial cut. Average compressive stresses were computed for each ROI and compared among the different configurations and motions. The micromotions between the implant and bone were also computed and compared.

Results

Kinematic Results

As shown in Table 2, both prosthesis models returned similar values for the max flexion-extension and abduction angles during lunge and squat. However, max internal-external rotation is considerably different between hinged and CCK because the latter does not allow this movement, thus maintaining this value below 1°.

Kinetic Results

The max contact forces during lunge and squat motions, calculated in the different joint regions, are reported in Table 3.

The lunge movement in the 2 prostheses led to different kinetic output; while analyzing the squat movement, the 2 models present almost similar contact forces except for the one related to the rotating pin and post-cam system.

Bone Stress Results

The compressive stress values in the tibial bone for each ROI analyzed are represented in Figure 2: for both motor tasks, the results are paired to allow a simpler comparison among the designs. A similar pattern in stress distributions can be found for each of the 4 configurations, but the values for the hinged usually tend to be higher than the CCK ones (this is due to the different level of constraint in the 2 models that led to different forces). The bone

Table 3
Max Contact Forces During Lunge and Squat Motions of the Hinged and CCK TKA.

Activity	Load Considered	Hinged TKA	CCK TKA
Lunge	Lateral tibiofemoral force	2798 N	1962 N
Lunge	Medial tibiofemoral force	1715 N	1823 N
Lunge	Patellar tendon force	3518 N	3268 N
Lunge	Rotating pin/post-cam force	1066 N	1110 N
Squat	Lateral tibiofemoral force	2143 N	1720 N
Squat	Medial tibiofemoral force	1429 N	1368 N
Squat	Patellar tendon force	3121 N	3073 N
Squat	Rotating pin/post-cam force	1099 N	1620 N

All the values reported in the table are in Newton.
CCK, condylar constrained knee; TKA, total knee arthroplasty.

stress tends to increase along the tibial bone up to the tip of the stem (ROIs, 17-18), after which it decreases for both designs. It is nonetheless possible to observe a peak of compression stress in the regions corresponding to the stem tip for the hinged model, while the CCK solution reports instead a stress reduction in the same areas: this is a consequence of the different design of the stems (Fig. 1), the CCK design presents a slotted stem while the hinged TKA presents an unslotted stem, acting thus as a stress riser.

Another section worthy of note is the proximal tibia (ROIs, 1-3), where the stress induced by the CCK appears to be higher than the one induced by the hinged, contrariwise to what happens in all the other regions. This is caused by the action of the post-cam mechanism, which leads to a more proximal distribution of the force than the hinged joint, and because of the internal-external constraint characteristic of this prosthesis design: indeed, conversely to the hinged (that allows rotation and therefore is not able to transmit any torsion to the bone), the CCK transfers all these loads to the immediately proximal area.

Micromotion Results

The micromotions, calculated as the relative displacement between the implant and the bone along the cutting plane, are reported in Figure 4 for all the analyzed configurations. Figure 3, instead, shows and compares the average compressive stress at bone-implant interface.

For each task, the CCK model presents higher values than the hinged solution as a consequence of the post-cam mechanism that, as previously reported, distributes the force more proximally compared to the hinged joint; the high interface stress generated, indeed, coupling the torque transferred to the underlying bone by the CCK and then leads to increased micromovements, as highlighted by the similarity between Figures 3 and 4.

Finally, in Figure 5 is illustrated the comparison among the stem axial displacement for the 2 models and movements; the CCK design returns higher displacement (up to 45%) compared to the hinged design and again this is a consequence of the slotted design of the stem, more flexible than the one of the hinged design and then subject to higher axial deformations.

Discussion

Little biomechanical information is nowadays available to compare the advantages/disadvantages of different level of constraint induced by TKA revision, as hinged and semiconstrained systems, during realistic dynamic activities. Thus, in this study such designs were compared during different motor tasks analyzing prosthesis forces and motion, tibial bone stresses, and implant micromotions.

The lunge movement in the 2 prostheses led to different kinetic output. The lateral and medial condylar forces result to be mostly higher in the hinged than in the CCK: this is due to the difference in the designs and in the constraints, as the hinged does not allow any anteroposterior translation and therefore it induces an increase in force. The max patellofemoral force instead appears to be similar in both prostheses, same as what happens for the ones in the rotating pin (for the hinged) and in the post-cam system (for the CCK).

Analyzing the squat movement, the 2 models present almost similar contact forces except for the one related to the rotating pin and post-cam system; in detail, the CCK force returns to be higher than during the lunge movement due to a greater anteroposterior pressure applied by the cam to the post, that is directly proportional to the rise in flexion angles.

Even if a validated model was adopted in the present work, several assumptions were made during the implementation of the FE models: first, the different structures are based on only one

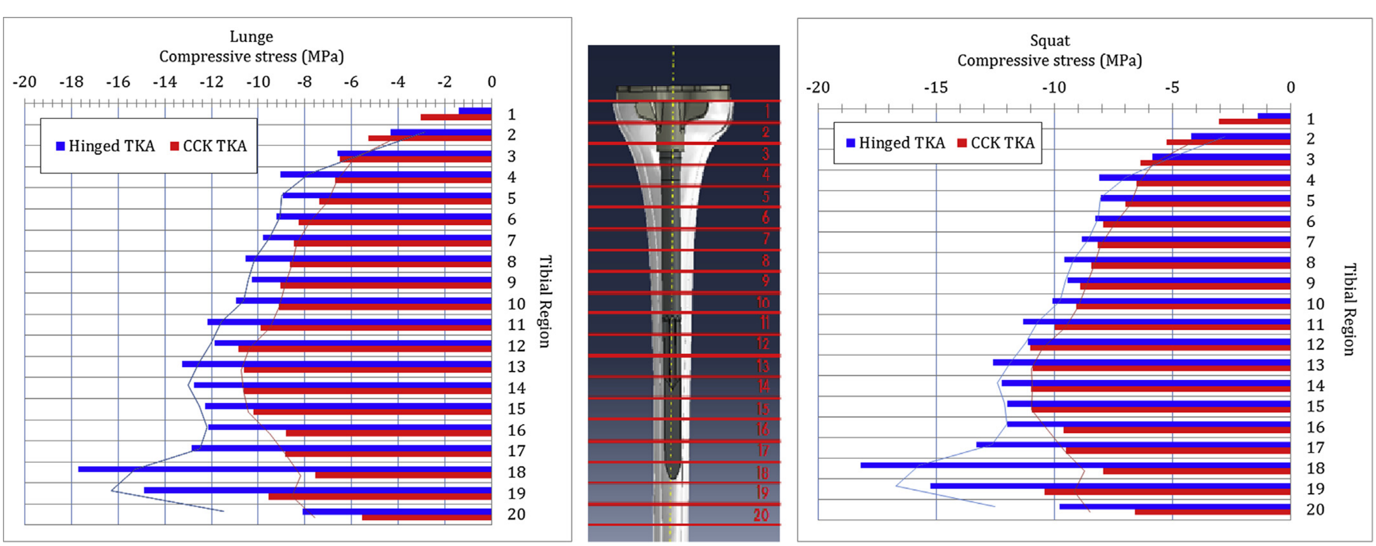

Fig. 2. Average compressive bone stress distribution for the hinged design (in blue) and for the semiconstrained design (in red): the left box corresponds to the lunge motor task, while the right box is related to the squat. Each bar reports the average stress value of a specific region of interest (from 1 to 20) analyzed along the tibia from the proximal to the distal region as illustrated in the central box. CCK, condylar constrained knee.

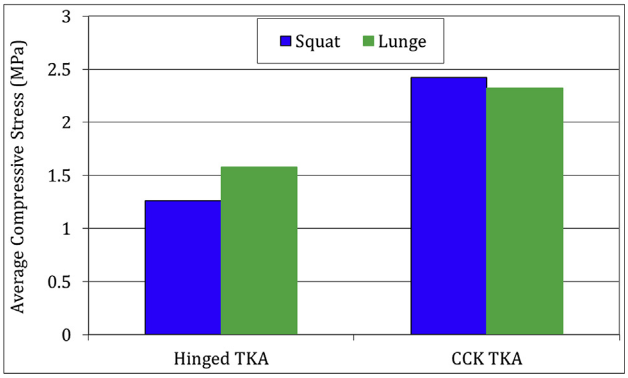

Fig. 3. Average compressive stress at the bone-implant interface for the 2 designs during the 2 motions (in blue the squat motion, in green the lunge motion).

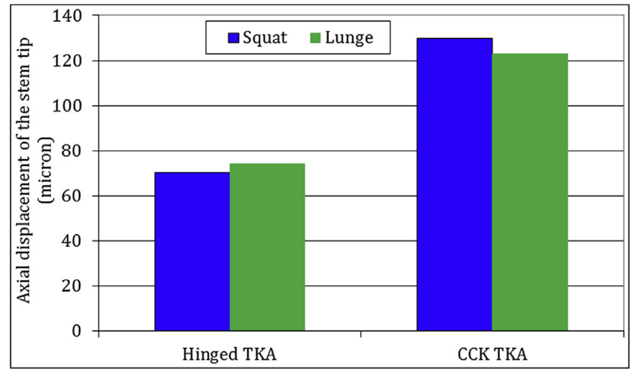

Fig. 5. Axial displacements for the 2 TKA solutions during the 2 performed tasks (in blue the squat, in green the lunge).

geometry so no variation in the anatomy of the specimen was taken in consideration; however, this approach has already been used in literature studies for similar knee biomechanical analyses [28,36,39,40]. Only one implant design was chosen to represent each level of constraint, but it is to be noted that the aim of the study was to compare 2 different constrain levels and not 2 specific designs. Furthermore, as no bone defect was considered in the study, no additional features (such as sleeves or cones) were modeled because their contribution was not required; this can therefore be integrated in future studies, however not compromising the relevance of the present activity. The heterogeneity of the cortical and cancellous bones, which could affect the stress results, was not considered in our model and eventual large bone defects or poor bone stock due to osteoporosis were not taken into account. In this study, cemented stem configurations were not considered, even if they represent a possible clinical solution; this decision was made as a study on this topic was previously published [40] showing that cemented stem induced lower stress distribution: as a consequence, press-fit stems were investigated as they represent the worst scenario in terms of implant-bone load sharing, allowing a better bone stress comparison between the 2 implant designs. Cadaveric studies and improved FE analysis could lead to future improvement of this comparison study on these category of implants.

Even if the presented findings are based upon the previously described assumptions, the results achieved in this study are a potential biomechanical explanation for the different behaviors observed in patients after surgery depending on which one of the 2 designs was adopted.

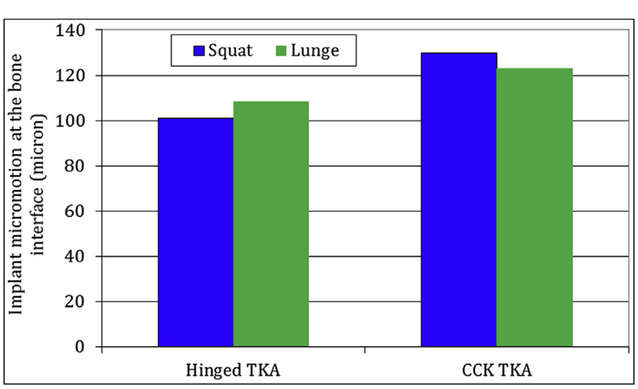

Fig. 4. Implant micromotions at the bone-implant interface for the 2 designs during the 2 motions (in blue the squat, in green the lunge).

Moreover, our results are in agreement with literature studies reported by different authors. Indeed, Walker et al [34] compared the performance of semiconstrained and RTH designs of TKA by mechanical testing, then by using the Knee Society clinical and radiographic evaluations and finally by a self-assessment questionnaire; the results from the questionnaire brought out a high correlation in the performances between the operated and non-operated knees in the RTH group, indicating that hinged designs were capable of matching their performance to a required level, thereby producing a better overall clinical result. The study indicated that a RTH should be taken in greater consideration in particular if its disadvantages related to larger bone resection and longer stems will be overcome. In agreement, the results of the present study showed trends that are dependent on the analyzed task in the semiconstrained solution, while the hinged TKA has a similar bone-stress and implant-micromotion patterns regardless of the motor task (Figs. 2-5).

Other studies [22] experienced the analysis of the changes in mineral bone density using the dual-energy X-ray absorption in primary TKA or after revision surgery [23], but only few used FE. As example, Quilez et al [24] tried to detect the best management of severe bone defects following TKA: they analyzed metal augments, tantalum cones, and porous tibial sleeves that could help the surgeon to manage any type of bone loss, providing a stable and durable knee joint reconstruction. In all cases, the bone density decreases in the proximal epiphysis and medullary channels, while an increase is predicted in the diaphysis and in the area surrounding the stems tips. The highest stress value has been obtained for the straight tibial stem, and the lowest for the stemless metaphyseal sleeve prosthesis.

In another study, conducted by means of FE modeling, Conlisk et al [25] concluded that patients with large femoral defects or severely compromised bone quality are particularly vulnerable to implant failure when a modular approach is adopted.

The main difference in stress that was observed in the present study is at the level of the stem tips (Fig. 2), but this could be attributed to the different shape of the stem itself. In fact, the hinged design presents an unslotted shape that is more rigid than the stem used for the CCK, the tip of which is reduced in volume because of the distal slot and is thus more flexible.

Regarding the proximal bone resorption, our results clearly highlights that the stress induced by the semiconstrained TKA is higher than the one induced by the hinged design in the proximal ROIs. These results can be due to the hinged implant that is also rotating, thus it cannot transmit torsional loads to the tibia bone, while the semiconstrained can distribute all the loads (force and torque) to the bone. The axial superior-inferior movement, furthermore, results to be higher (up to 45%) for the semiconstrained solution compared to the hinged design. The hinged prosthesis allows, during flexion, an internal-external rotation of approximately 10° each, constrained at 0° by the tibial polyethylene insert when in full extension. According to the peg design, this prosthesis allows superior-inferior displacement between femoral and tibial components, nonetheless avoiding any implant dislocation. The femoral component can lift off the tibial polyethylene insert when extremely flexed, which decreases the axial forces, reducing the proximal bone stress.

The increased stress in the CCK is a consequence of the post-cam constraint: in fact, the anteroposterior force increases with flexion [3,4] and consequently is transmitted by the post-cam mechanism, hence generating a lever arm that will greatly load the proximal tibia. Contrariwise, the hinged design will transmit the stress to a more distal region in the tibia, leading then to a more gradual stress distribution on the bone, thanks to the RTH pin.

In conclusion, this study could help to define the best compromise between the 2 revision TKA in terms of management of bone loss, ligament laxity, and implant stability during surgery and to achieve a better force distribution on residual bone, in order to provide a greater stability and a durable implant performance. Surgeons will have to consider these findings to guarantee the best outcome for the patient and the related change in the bone stress and implant fixation induced by different levels of constrain in a TKA.

Acknowledgments

This work was supported by FNRS, Belgium (Fonds National de la Recherche Scientifique, CDR 19545501) and by FER ULB (Fonds d'Encouragement a la Recherche, FER 2014). The funders had no role in study design, data collection and analysis, decision to publish, or preparation of the manuscript.

References

[1] Sharkey PF, Hozack WJ, Rothman RH, Shastri S, Jacoby SM. Insall award paper: why are total knee arthroplasty failing today? Clin Orthop Relat Res 2002;404:7–13.
[2] Sharkey PF, Lichstein PM, Shen C, Tokarski AT, Parvizi J. Why are total knee arthroplasties failing today—has anything changed after 10 years? J Arthroplasty 2014;29:1774–8.
[3] Indelli PF, Giori N, Maloney W. Level of constraint in revision knee arthroplasty. Curr Rev Musculoskelet Med 2015;8:390–7.
[4] Kurtz S, Ong K, Lau E, Mowat F, Halpern M. Projections of primary and revision hip and knee arthroplasty in the United States from 2005 to 2030. J Bone Joint Surg Am 2007;89:780–5.
[5] Vasso M, Beaufils P, Schiavone Panni A. Constraint choice in revision knee arthroplasty. Int Orthop 2013;37:1279–84.
[6] Malcolm TL, Bederman SS, Schwarzkopf R. Outcomes of varus-valgus constrained versus rotating-hinge implants in total knee arthroplasty. Orthopedics 2016;39:e140–8.
[7] Hommel H, Wilke K, Kunze D, Hommel P, Fennema P. Constraint choice in revision knee arthroplasty: study protocol of a randomised controlled trial assessing the effect of level of constraint on postoperative outcome. BMJ Open 2017;7:e012964.
[8] Das S, Arkesh M, Selvanayagam R. Constraints in total knee arthroplasty: current status and review of literature. Int J Res Med Sci 2017;5:374–8.
[9] Lettin AW, Deliss LJ, Blackburne JS, Scales JT. The Stanmore hinged knee arthroplasty. J Bone Joint Surg Br 1978;60:327–32.
[10] Deburge A, Guepar. Guepar hinge prosthesis: complications and results with two years' follow-up. Clin Orthop Relat Res 1976;120:47–53.
[11] Walker PS, Emerson R, Potter T, Scott R, Thomas WH, Turner RH. The kinematic rotating hinge: biomechanics and clinical application. Orthop Clin North Am 1982;13:187–99.
[12] McAuley JP, Engh GA. Constraint in total knee arthroplasty: when and what? J Arthroplasty 2003;18:51–4.
[13] Jones RE. Total knee arthroplasty with modular rotating platform hinge. Orthopedics 2009;29:S80–2.
[14] Sculco TP. The role of constraint in total knee arthroplasty. J Arthroplasty 2006;21:54–6.
[15] Morgan H, Battista V, Leopold SS. Constraint in primary total knee arthroplasty. J Am Acad Orthop Surg 2005;13:515–24.
[16] Hwang SC, Kong JY, Nam DC, Kim DH, Park HB, Jeong ST, et al. Revision total knee arthroplasty with a cemented posterior stabilized, condylar constrained or fully constrained prosthesis: a minimum 2-year follow-up analysis. Clin Orthop Surg 2010;2:112–20.
[17] Kafidas D, Karachalios T. Long term outcome of total knee arthroplasty rotating hinge designs. In: Karachalios T, editor. Total knee arthroplasty. London: Springer; 2015. p. 179–91.
[18] Draganich LF, Whitehurst JB, Chou L, Piotrowski GA, Pottenger LA, Finn HA. The effects of the rotating-hinge total knee replacement on gait and stair stepping. J Arthroplasty 1999;14:743–55.
[19] Gudnason A, Milbrink J, Hailer NP. Implant survival and outcome after rotating-hinge total knee revision arthroplasty: a minimum 6-year follow-up. Arch Orthop Trauma Surg 2011;131:1601–7.
[20] Barrack RL, Lyons TR, Ingraham RQ, et al. The use of a modular rotating hinge component in salvage revision total knee arthroplasty. J Arthroplasty 2000;15:858–66.
[21] Neumann DR, Hofstaedter T, Dorn U. Follow-up of a modular rotating hinge knee system in salvage revision total knee arthroplasty. J Arthroplasty 2012;27:814–9.
[22] Gehrke T, Kendoff D, Haasper C. The role of hinges in primary total knee replacement. Bone Joint J 2014;96-B:93–5.
[23] Joshi N, Navarro-Quilis A. Is there a place for rotating-hinge arthroplasty in knee revision surgery for aseptic loosening? J Arthroplasty 2008;23:1204–11.
[24] Hossain F, Patel S, Haddad FS. Midterm assessment of causes and results of revision total knee arthroplasty. Clin Orthop Relat Res 2010;468:1221–8.
[25] Wilke K, Kunze D, Hommel P, Hommel H. Rotating hinge total knee arthroplasty RT-PLUS solution: a clinical and radiographic follow-up. J Orthopedics Rheumatol 2016;3:4.
[26] Dall'Oca C, Ricci M, Vecchini E, Giannini N, Lamberti D, Tromponi C, et al. Evolution of TKA design. Acta Biomed 2017;88:17–31.
[27] Pianigiani S, Bernabé RA, Yagüe HR, Innocenti B. Investigation on the effects induced by TKA features on tibio-femoral mechanics part II: tibial insert designs. J Mech Med Biol 2015;2:1540035.
[28] Pianigiani S, Scheys L, Labey L, Pascale W, Innocenti B. Biomechanical analysis of the post-cam mechanism in a TKA: comparison between conventional and semi-constrained insert designs. Int Biomech 2015;2:22–8.
[29] Anderson JA, Baldini A, MacDonald JH, Tomek I, Pellicci PM, Sculco TP. Constrained condylar knee without stem extensions for difficult primary total knee arthroplasty. J Knee Surg 2007;20:195–8.
[30] Lachiewicz PF, Soileau ES. Results of a second-generation constrained condylar prosthesis in primary total knee arthroplasty. J Arthroplasty 2011;26:1228–31.
[31] Kim YH, Kim JS. Revision total knee arthroplasty with use of a constrained condylar knee prosthesis. J Bone Joint Surg Am 2009;91:1440–7.
[32] Arnout N, Vanlommel L, Vanlommel J, Luyckx JP, Labey L, Innocenti B, et al. Post-cam mechanics and tibiofemoral kinematics: a dynamic in vitro analysis of eight posterior-stabilized total knee designs. Knee Surg Sports Traumatol Arthrosc 2015;23:3343–53.
[33] Fuchs S, Sandmann C, Gerdemann G, Skwara A, Tibesku CO, Bottner F. Quality of life and clinical outcome in salvage revision total knee replacement: hinged vs total condylar design. Knee Surg Sports Traumatol Arthrosc 2004;12:140–3.
[34] Walker PS, Manktelow AR. Comparison between a constrained condylar and a rotating hinge in revision knee surgery. Knee 2001;8:269–79.
[35] Pianigiani S, Innocenti B. The use of finite element modeling to improve biomechanical research on knee prosthesis. In: New developments in knee prosthesis research. Hauppauge, NY: Nova Science Publishers, Inc; 2015.
[36] Innocenti B, Bilgen OF, Labey L, van Lenthe HG, Vander Sloten J, Catani F. Load sharing and ligament strains in balanced, overstuffed and understuffed UKA. A validated finite element analysis. J Arthroplasty 2014;29:1491–8.
[37] Brihault J, Navacchia A, Pianigiani S, Labey L, De Corte R, Pascale V, et al. All-polyethylene tibial components generate higher stress and micromotions than metal-backed tibial components in total knee arthroplasty. Knee Surg Sports Traumatol Arthrosc 2016;24:2550–9.
[38] Innocenti B, Truyens E, Labey L, Wong P, Victor J, Bellemans J. Can medio-lateral baseplate position and load sharing induce asymptomatic local bone resorption of the proximal tibia? A finite element study. J Orthop Surg Res 2009;4:26.
[39] Innocenti B, Bellemans J, Catani F. Deviations from optimal alignment in TKA: is there a biomechanical difference between femoral or tibial component alignment? J Arthroplasty 2016;31:295–301.
[40] El-Zayat BF, Heyse TJ, Fanciullacci N, Labey L, Fuchs-Winkelmann S, Innocenti B. Fixation techniques and stem dimensions in hinged total knee arthroplasty: a finite element study. Arch Orthop Trauma Surg 2016;136:1741–52.
[41] Barrack R, Rorabeck C, Burt M, Sawhney J. Pain at the end of the stem after revision total knee arthroplasty. Clin Orthop Relat Res 1999;367:216–25.
[42] Barrack RL, Stanley T, Burt M, Hopkins S. The effect of stem design on end-of-stem pain in revision total knee arthroplasty. J Arthroplasty 2004;19:119–24.
[43] Ingrassia T, Nalbone L, Nigrelli V, Tumino D, Ricotta V. Finite element analysis of two total knee prostheses. Int J Interact Des Manuf 2013;7:91–101.

[44] Sarathi Kopparti P, Lewis G. Influence of three variables on the stresses in a three-dimensional model of a proximal tibia-total knee implant construct. Biomed Mater Eng 2007;17:19–28.
[45] Innocenti B, Pianigiani S, Ramundo G, Thienpont E. Biomechanical effects of different varus and valgus alignments in medial unicompartmental knee arthroplasty. J Arthroplasty 2016;31:2685–91.
[46] Soenen M, Baracchi M, De Corte R, Labey L, Innocenti B. Stemmed TKA in a femur with a total hip arthroplasty: is there a safe distance between the stem tips? J Arthroplasty 2013;28:1437–45.
[47] Vaninbroukx M, Labey L, Innocenti B, Bellemans J. Cementing the femoral component in total arthroplasty: which technique is the best? Knee 2009;16: 265–8.
[48] Vanlommel J, Luyckx JP, Labey L, Innocenti B, De Corte R, Bellemans J. Cementing the tibial component in total knee arthroplasty: which technique is the best? J Arthroplasty 2011;26:492–6.
[49] Simpson DJ, Little JP, Gray H, Murray DW, Gill HS. Effect of modular neck variation on bone and cement mantle mechanics around a total hip arthroplasty stem. Clin Biomech 2009;24:274–85.
[50] Innocenti B, Pianigiani S, Labey L, Victor J, Bellemans J. Contact forces in several TKA designs during squatting: a numerical sensitivity analysis. J Biomech 2011;44:1573–81.
[51] Pianigiani S, Chevalier Y, Labey L, Pascale V, Innocenti B. Tibio-femoral kinematics in different total knee arthroplasty designs during a loaded squat: a numerical sensitivity study. J Biomech 2012;45:2315–23.
[52] Pianigiani S, Labey L, Pascale W, Innocenti B. Knee kinetics and kinematics: what are the effects of TKA malconfigurations? Knee Surg Sports Traumatol Arthrosc 2016;24:2415–21.
[53] Grood ES, Suntay WJ. A joint coordinate system for the clinical description of three-dimensional motions: application to the knee. J Biomech Eng 1983;105: 136–44.